BIOCHEMICAL PHARMACOLOGY 75 (2008) 2276–2288

available at www.sciencedirect.com

ScienceDirect

journal homepage: www.elsevier.com/locate/biochempharm

Analysis of changes in the proteome of HL-60 promyeloid leukemia cells induced by the proteasome inhibitor PSI

Mi-Ran Choi [a,b], Farhad Najafi [b], Ahmad R. Safa [b], Hannes C.A. Drexler [a,*]

[a] Max Planck Institute for Molecular Biomedicine, Department for Vascular Cell Biology, Roentgenstr. 20, 48149 Muenster, Germany
[b] Department of Pharmacology and Toxicology and The Indiana University Cancer Center, 1044 West Walnut Street R4-132, Indianapolis, IN 46202, USA

ARTICLE INFO

Article history:
Received 5 February 2008
Accepted 20 March 2008

Keywords:
Proteasome inhibitor
Apoptosis
Multidrug resistance
P-gp
MDR-1

ABSTRACT

Proteasome inhibitors display potent anti-neoplastic and anti-angiogenic properties both in vitro and in vivo. The mechanisms, however, by which proteasome inhibitors kill tumor cells are still fairly elusive as is the molecular basis of resistance to treatment. To address these questions, we employed a high-throughput Western blotting procedure to analyze changes in a subproteome of ~800 proteins in the promyelocytic leukemia cell line HL-60 upon treatment with the proteasome inhibitor PSI (Z-Ile-Glu(OtBu)-Ala-Leu-aldehyde) and correlated the changes of selected target proteins with the changes in two multidrug-resistant HL-60 variants. In total, 105 proteins were upregulated more than 1.5-fold after PSI treatment, while 79 proteins were downregulated. Activation of caspases-3 and -8, modulation of members of the Bcl-2 family as well as stimulation of stress signaling pathways was prominent during HL-60 apoptosis. We also identified changes in the abundance of proteins previously not known to be affected by proteasome inhibitors. In contrast, two multidrug-resistant HL-60 cell lines, overexpressing either MRP1 or P-glycoprotein were largely resistant to PSI-induced apoptosis and could not be resensitized by the pharmacological inhibitors of the drug efflux pumps MK571 or PSC833. Drug resistance was also independent of the upregulation of Bad. Overexpression of multidrug resistance proteins, P-glycoprotein and MRP-1 is thus not sufficient to explain resistance of HL-60 cells to treatment with proteasome inhibitor PSI, which remains more closely related to a low level of Bax expression and to the inability to activate JNK. Alternative routes to the acquisition of resistance to PSI have therefore to be considered.

© 2008 Elsevier Inc. All rights reserved.

1. Introduction

Inhibition of proteasome function by low molecular weight inhibitors has been shown to induce cell cycle arrest and apoptosis preferentially in transformed or rapidly proliferating cells [1–3] and to sensitize tumor cells to radiotherapy [4] as well as to the cytotoxic action of various conventional chemotherapeutic compounds [5–11]. Following observations in preclinical tumor models, which revealed potent anti-neoplastic and anti-angiogenic properties of proteasome inhibitors also in vivo [5,12–14], bortezomib (PS-341, Velcade®) has recently been approved as the first novel in class proteasome inhibitor for its use in patients suffering from refractory and relapsed multiple myeloma [15]. In addition, bortezomib has entered various clinical trials since then in which the potency of this anticancer drug either as single

* *Corresponding author*. Tel.: +49 251 70365248; fax: +49 251 70365299.
E-mail addresses: mirchoi@iupui.edu (M.-R. Choi), fnajafi@iupui.edu (F. Najafi), asafa@iupui.edu (A.R. Safa), hannes.drexler@mpi-muenster.mpg.de (Hannes C.A. Drexler).
0006-2952/$ – see front matter © 2008 Elsevier Inc. All rights reserved.
doi:10.1016/j.bcp.2008.03.017

agent or in combination with other chemotherapeutics is being evaluated [16]. The success of bortezomib, which has established the principle of proteasome inhibition as a novel cancer treatment modality, has further promoted the development of more novel proteasome inhibitors, such as NPI-0052 [17,18] or PR-171 [19], which show increased activity, reduced toxicity and enhanced oral availability (NPI-0052).

The relative efficacy of proteasome inhibitors to induce apoptosis in particular tumor cell types can be explained by the fact that the effect of blocking proteasome function is not monospecific but rather targets the half-life of a multitude of proteins involved in metabolic, transcriptional or signaling pathways critical for cell survival. Prominent events in proteasome inhibitor-induced apoptosis include the production of reactive oxygen species (ROS) [20,21], activation of the stress kinases JNK [22–24] and p38 [8,10,25,26] as well as abrogation of cytoprotective p42/p44 MAPK signaling [27,28]. Furthermore, transcriptional activation of NFκB dependent survival promoting genes, such as cIAP-1 and cIAP-2 [29], XIAP [30], A1 and A20 [31,32] and Bcl-xL [33] is inhibited by blocking the degradation of IκB [34,35]. Mutations in the canonical or alternative pathways of NFκB-activation, which lead to chronic activation of this transcription factor, have been shown to occur quite frequently in tumor cells [36]. Many cell lines for instance that are derived from multiple myeloma patients and in which the proteasome inhibitor bortezomib has displayed convincing therapeutic efficacy, harbor constitutively active NFκB and are therefore critically dependent on NFκB activity for survival [37,38].

However, it is becoming increasingly clear that not all tumor types are equally sensitive to treatment with proteasome inhibitor such as breast cancer [39], renal cell cancer [40] or melanoma [41], and that there is a substantial fraction of myeloma patients who do not respond to bortezomib therapy or who relapse following treatment [42]. Although some players of proteasome inhibitor-mediated cytotoxicity have been identified as indicated above, the mechanisms of drug resistance remain poorly understood.

Since proteasome inhibitors interfere with protein turnover by either stabilizing proteins post-translationally or by modulating expression levels by transcriptional activation or repression, we used a high-throughput immunoblotting approach to identify changes in the subproteome of HL-60 promyeloid leukemia cells that might be critically involved in proteasome inhibitor mediated apoptosis and the development of drug resistance.

2. Materials and methods

2.1. Cell culture and reagents

The acute promyelocytic leukemia cell line HL-60 as well as the MRP1-overexpressing variant HL-60/ADR cell line [43] and the MDR1-overexpressing multidrug-resistant derivative HL-60/VCR [44] were maintained in RPMI-1640 containing 10% heat-inactivated fetal calf serum, supplemented with penicillin and streptomycin (Life Technologies, Grand Island, NY, USA) at 37 °C in humidified air with 5% CO_2. HL-60/ADR and HL-60/VCR cells were grown in the presence of 5 μg/ml doxorubicin (DOX) and 1 μg/ml vincristine (VCR), respectively. The drugs were removed from the media a week before performing experiments.

Proteasome inhibitor PSI (N-carbobenzoxy-L-isoleucyl-L-γ-t-butyl-L-glutamyl-L-alanyl-L-leucinal) was obtained from Peptide Institute (Osaka, Japan) and dissolved in DMSO at a concentration of 50 mM. Stock solutions were stored at −20 °C and diluted into tissue culture medium to a final concentration of 0.1 μM, 1 μM or 50 μM. Vincristine (VCR) was obtained from Eli Lilly and Co. (Indianapolis, IN, USA) and doxorubicin (DOX) was purchased from Sigma Chemical Co. (St. Louis, MO, USA) as were all other chemicals unless stated otherwise. Doxorubicin and vincristine were dissolved in sterile H_2O at a concentration of 0.1 mg/ml and diluted into culture medium to the final concentration. P-glycoprotein inhibitor PSC833 was a gift of Elli Lilly and Co. (Indianapolis, IN, USA) and MRP-1 inhibitor MK571 was purchased from Alexis (San Diego, CA, USA). PSC833 and MK571 were dissolved in DMSO at a concentration of 10 mM and 80 mM, respectively. Stock solutions were diluted into culture medium to a final concentration of 3 μM and 30 μM, respectively.

2.2. High-throughput immunoblotting

The high-throughput immunoblot screening, in which cell lysates are analyzed against a panel of 800 well-characterized antibodies was performed by BD Biosciences Transduction Laboratories (PowerBlot; Lexington, KY, USA). 5×10^6 HL-60 cells in 10 ml growth medium were incubated with 50 μM PSI for 6 h or 15 h to induce apoptosis. An equal number of control cells were incubated with DMSO for 15 h. The final concentration for DMSO did not exceed 0.1% in any sample. Apoptotic- and non-apoptotic HL-60 cells were harvested by centrifugation and washed once with cold PBS. Cell pellets were resuspended in 0.6 ml of boiling SDS lysis buffer (10 mM Tris·HCl pH 7.4, 1 mM sodium orthovanadate, 1% SDS), briefly microwaved (5–10 s) and homogenized by passing the lysate 10 times through a 26 G needle. Protein concentrations were determined using a BCA assay (Pierce; Rockford, IL, USA). Protein samples were diluted to 1 mg/ml final concentration with 2× electrophoresis loading buffer (125 mM Tris·HCl pH 6.8, 4% SDS, 10% glycerol, 0.006% bromophenol blue, 2% β-mercaptoethanol) and subjected to PowerBlot Western analysis.

For each sample, five SDS-gels were run (500 μg protein/gel) and transferred to Immobilon membranes. Each blot divided into 45 lanes was probed with 160 antibodies in a multiplexed fashion (4 antibodies per lane/channel). As secondary antibodies peroxidase-coupled anti-mouse antibodies were used. Blots were developed using the SuperSignal reagent (Pierce; Rockford, IL, USA). Blot images were then captured digitally and normalized. The ratio between control and treated samples was determined and changes were expressed as fold increase or decrease. Protein expression changes were summarized in five confidence levels, determined by signal intensity, fold change and reproducibility (level 5: changes >2-fold in triplicate from good quality signals; level 4: changes 1.50–1.99-fold in triplicate from good quality signals; level 3: changes 1.25–1.49-fold in triplicate from good quality signals; level 2: changes <1.25-fold in triplicate from low signals; and

level 1: changes >2-fold in duplicate from good quality signals).

2.3. Conventional Western blot analysis

4×10^6 cells of HL-60, HL-60/ADR and HL-60/VCR cells were treated with 50 μM PSI for 15 h. Cells were lysed in SDS lysis buffer (10 mM Tris·HCl pH 7.4, 1 mM sodium orthovanadate, 1% SDS). Protein concentration was determined by BCA assays (Pierce; Rockford, IL, USA). Equal amount of protein samples were separated on NuPAGE 4–12% Bis–Tris gels (Invitrogen; Carlsbad, CA) and transferred to PVDF membrane (Immobilon-P, Milipore; Bedford, MA, USA). The surface of the membrane was blocked in PBST-buffer (PBS, pH 7.5 and 0.1% Tween20) containing 5% nonfat milk. Primary antibodies were purchased from Santa Cruz (caspases-1–8, Bad, Bax, Bcl-2, Bid, c-Jun and phospho-JNK; Santa Cruz, CA, USA); antibodies directed against 14-3-3 were obtained from BD PharMingen (San Diego, CA, USA). Antibodies were diluted in 5% nonfat milk-PBST buffer and incubated at room temperature or over night at 4 °C. Horseradish peroxidase-conjugated anti-mouse, anti-rabbit antibodies (Amersham Biosciences; Piscataway, NJ, USA) or anti-goat antibodies (Santa Cruz; Santa Cruz, CA, USA) were used as secondary antibodies. Proteins were detected by chemiluminescence (SuperSignal; Pierce; Rockford, IL, USA).

2.4. Apoptosis assays

For apoptosis assay, 0.2×10^6 cells of HL-60 in 2 ml growth medium were incubated with proteasome inhibitor PSI at a final concentration of 0.1 μM, 1 μM and 50 μM. HL-60/ADR and HL-60/VCR cells at a same cell density were incubated with 50 μM PSI for 15 h. Control cells received DMSO only. The final concentration of DMSO did not exceed 0.1%. After incubation, the cells were co-stained with Annexin-V-FITC and propidium iodide (PI). The numbers of early apoptotic (Annexin-V-FITC$^+$, PI$^-$) cells as well as late apoptotic (Annexin-V-FITC$^+$, PI$^+$) cells were determined by flow cytometry using a BD FACS Scan and BD cell quest software (BD Bioscience; San Diego, CA, USA).

3. Results

3.1. Apoptosis induction mediated by proteasome inhibitor PSI in HL-60 cells

Blockage of proteasomal function represents a post-translational event that should affect the half-life of numerous proteins, and we reasoned therefore that we might be able to identify important players of survival regulation in HL-60 cells by closely monitoring changes in the proteome of these cells upon proteasome inhibitor-mediated apoptosis. For this purpose we exploited the PowerBlot high-throughput Western blotting system, which allows detection of about 800 proteins (BD Transduction Laboratories; Lexington, KY, USA). To establish optimal conditions for the screening procedure, we determined in a first set of experiments apoptosis induction by the proteasome inhibitor PSI in HL-60 cells. As shown in Fig. 1, PSI induced cell death in HL-60 cells in a time- and dose-dependent manner (Fig. 1). Apoptosis by PSI administered at a concentration of 50 μM increased over 24 h and killed 83% of HL-60 cells. PSI-mediated cytotoxicity was also observed at a 500-fold lower concentration (0.1 μM), albeit with comparatively slower kinetics. Lysates were therefore generated from apoptotic HL-60 cells, that were incubated for 15 h with 50 μM PSI, which resulted in the induction of approximately 60% of apoptosis (>IC_{50}). In addition, lysates from HL-60 cells that had received PSI (50 μM) for 6 h were also included in our analysis to observe changes occurring during the early phase of apoptosis induction.

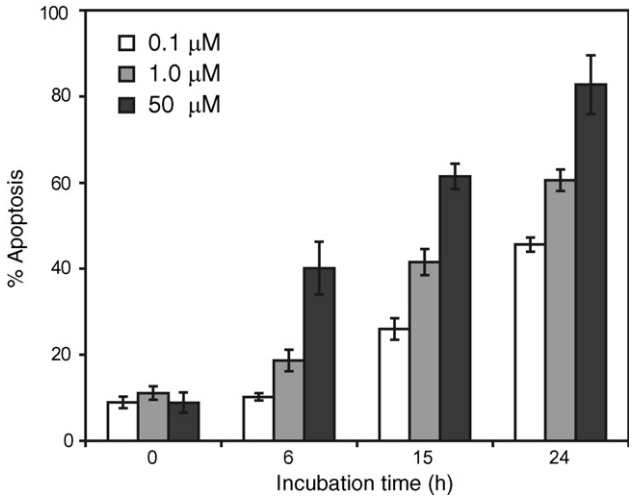

Fig. 1 – Time- and dose-dependent apoptosis induction by the proteasome inhibitor PSI. HL-60 cells were treated with 0.1 μM, 1.0 μM and 50 μM PSI for 6 h, 15 h and 24 h. Control cells received 0.1% DMSO. The amounts of apoptotic cells were determined after staining of the cells with Annexin-V-FITC and PI by flow cytometry. The percentages of apoptosis presented are the sum of early (Annexin-V-FITC$^+$ and PI$^-$) and late (Annexin-V-FITC$^+$ and PI$^+$) apoptotic cells. Shown are the mean values ± S.D. of six independent experiments.

3.2. Modulated expression of proteins during proteasome inhibitor-mediated apoptosis

A representative blot from PSI-treated cells is shown in Fig. 2. A total of 105 proteins were upregulated more than 1.5-fold (confidence levels 5 and 4) and 79 proteins were downregulated after 15 h of incubation with 50 μM PSI compared to DMSO-treated controls (Fig. 3). Additional 33 proteins were up- or downregulated, when including changes within confidence levels 3 and 2.

Alterations in protein expression levels became evident already after 6 h of exposure to PSI: 52 proteins were increased relative to the DMSO control, whereas 50 proteins showed reduced levels (confidence level 5–2; Fig. 4). All raw data as well as background information on the individual proteins that were detected under the described conditions are provided as supplementary tables in Excel format (15 h sample: supplementary Table S1; 6 h sample: supplementary Table S2).

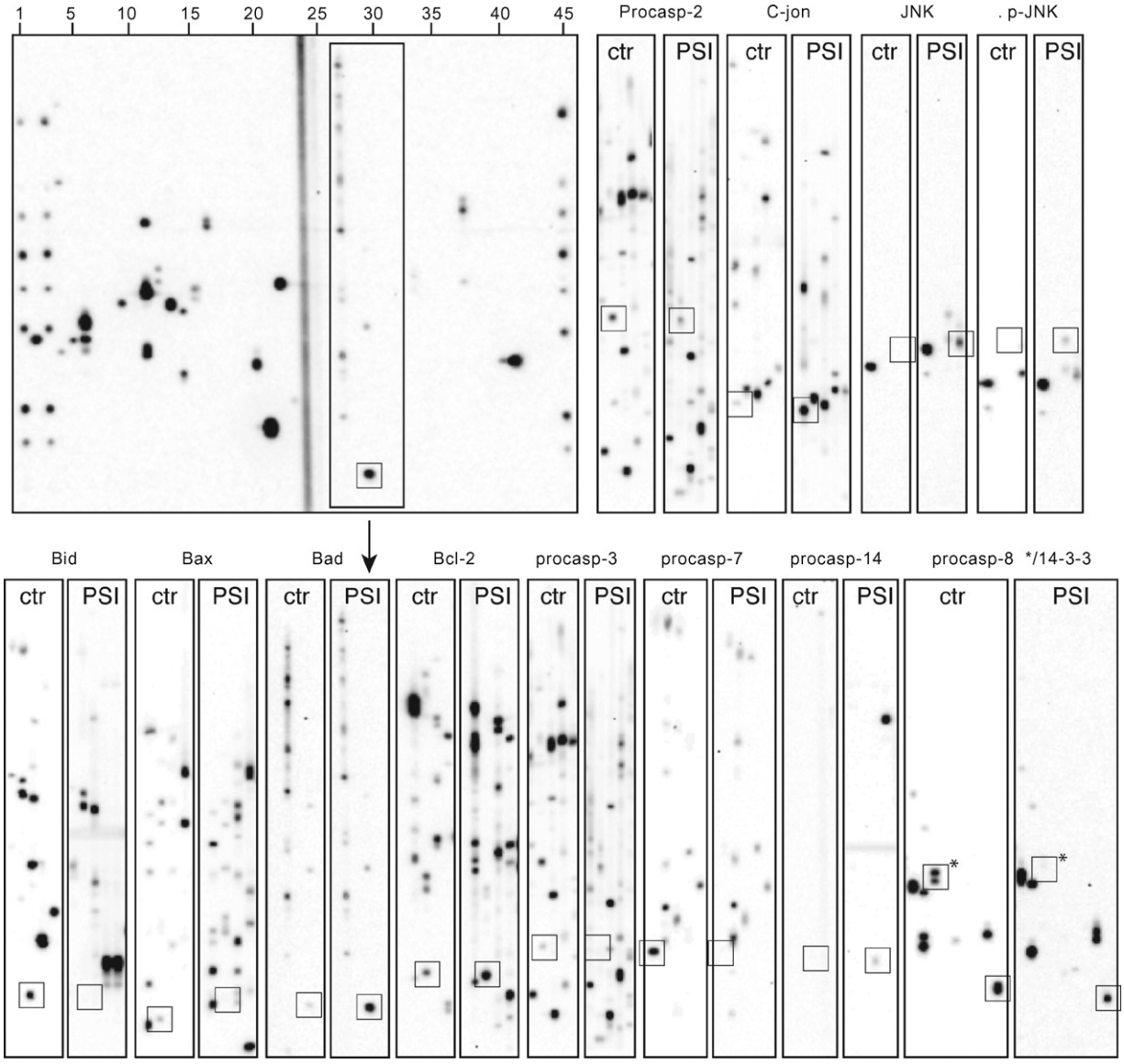

Fig. 2 – PowerBlot analysis of total protein from untreated and PSI-treated HL-60 cells. Protein samples were prepared as described in Section 2 following incubation of HL-60 cells with DMSO or with PSI (N-carbobenzoxy-L-isoleucyl-L-γ-t-butyl-L-glutamyl-L-alanyl-L-leucinal; 50 μM) for 6 h or 15 h. Samples were analyzed by high throughput multiplex Western blotting against a panel of 800 antibodies (PowerBlot®) as described. An example of such a blot (PSI-treated sample) is shown in the upper left corner. Selected proteins with altered expression levels are highlighted by squares. The molecular weight standard consisted of an antibody cocktail containing antibodies directed against P190 glued, Adaptin beta, STAT-3, PTP1D, Mek-2, RACK-1, GRB-2 and Rap2 (lane 1 and 45 in upper left panel). Blot images were digitally captured and analyzed by densitometry.

High-throughput immunoblotting confirmed several observations that have been previously described to occur as a consequence of exposure to proteasome inhibitors. These are related to increased expression of heat shock proteins (Hsp40) and of genes associated with stress signaling (p38 MAPK, heme oxygenase, MnSOD, Phospho-JNK, BiP/grp78), modulation of JAK/STAT signaling, with JAK1 and STAT1 being induced whereas levels of STAT3 and 5 were reduced. In addition, upregulation of components of the ubiquitin–proteasome degradation pathway has been reported earlier (Nedd4, Ubc9, Cul3) as well as sensitization to apoptosis induction by the extrinsic pathway (FADD, FasL, TRADD).

In contrast, other changes such as the upregulation of various kinases (Btk, C-Raf, CK1e, GSK3b, IKKγ, ILK, Lyn, MEK5, PI3K p110d, PKAc, PKB, PKCa, Yes, c-Cbl) and phosphatases (PP1, PP2C, PTP1C, CD45) had not been noted in previous proteomic studies (compare with [6,50]), which could have been due to cell type- and reagent-specific differences, since other cell types (multiple myeloma or megakaryoblastic leukemia cells) and different proteasome inhibitors (bortezo-

Protein	mean
Confidence Level 5	
ASS-low	5.54
Bcl-2	3.45
BPntase	2.11
Btk	2.93
c-Raf-1	p
CA150	17.60
CART1	17.51
Casein Kinase I epsilon	p
Caspase-14	p
Cathepsin D-43.8	p
CD45	12.59
CDC27	p
Cdk4	p
Chk1	5.69
Clathrin Heavy Chain-106.3	p
Clathrin Heavy Chain-23.6	p
CRP1	p
Cyclin D3	p
Cytochrome c	p
DBP2-107?	p
DHFR	14.08
drp1-25.2	p
Dystrobrevin	p
Ercc-1	p
FADD	p
Fas Ligand	3.68
G alpha t	p
Gap1m	p
GluR delta 2	p
GS15	9.82
hcKrox	3.99
Heme Oxygenase 1	p
hmSH3	p
HSF4	6.17
HsORC4	4.63
Hsp40	p
IKK gamma-44.5	5.30
ILK	p
IQGAP1	p
Jun	17.05
KAP-21.6	p
Kip1/p27	p
LAP2-low	7.23
LEDGF	p
MCM6	29.53
MEK5-45	p
mEPHX	p
Metaxin	12.87
MnSOD	p
Munc-18	p
Mxi-1	p
NAT1	p
Nedd4	p
NHE-1	p
Nip1	5.51

Protein	mean
Confidence Level 5	
NKT-122	p
NTF2	p
p160	p
Pax-5	p
Phospho-JNK	p
PI3-K p110 delta	p
pICln-41.2	20.47
PKB alpha/Akt	p
PKC alpha	3.04
PP1	3.54
PP2C delta	11.38
PRK2	p
R-Cadherin	p
Rab11-21.8	p
Rab11-23.4	5.70
Rab27	10.72
Rac1	p
Rap1	p
Rap2-22.6	3.89
Rho	13.94
Rin1-47.5	3.55
rSec8	3.01
Selenoprotein P-52.3	p
ShcC-55	p
SIII p15	p
Stat1 (C-terminus)-84.7	p
TFII-I-low	p
Tim23	4.80
TRADD	3.59
Ubc9	17.25
XPA	2.32
Confidence level 4	
Annexin VI	14.26
Bad	18.00
Cyclin B	3.33
ERK1	3.44
Fnk	8.84
GSK-3 beta	p
HES1	2.41
I kappa B alpha	1.90
JAK1-118.7	p
Kanadaptin	3.11
Lyn	2.39
MCM5	2.26
Mint1	p
Ndr	2.78
pan ERK-43.7	2.95
PARP	2.92
PKA C	3.71
Stat1 (C-terminus)	3.30
TIEG2	2.15
VASP(47)	10.59

Protein	mean
Confidence level 5	
14-3-3	4.67
53BP2	a
ABP-280	a
Acetylcholine Receptor alpha	a
Adaptin alpha	3.70
APM	a
B2 Bradykinin Receptor-42	4.31
Bax	20.84
Bid	a
Btf	a
Caspase 8	a
Caspase-2/ICH-1L	a
Caspase-7/MCH-3	a
CD100	a
DFF45	a
DSIF	2.29
Dynactin	a
Dynamin	4.20
Eg5	4.85
Endopeptidase 3.4.24.16	a
ERK2	4.45
FAK	a
FBP	45.23
Flotillin-2/ESA	16.31
GDNFR-alpha-49	95.89
GFAP	3.37
HES1	a
hHR23B	a
hILP/XIAP	4.00
hRAD9	a
HRF	5.49
HS1	7.54
I kappa B epsilon	a
Integrin alpha v	a
Itch	a
KAP-36.5	3.05
La Protein	73.09
LAP2	4.01
MAP2B	a
MAPKp49	5.57
MEK1	a
MEK2	4.95
MKP2	27.08
MSH6	a
MST1	a
NKT-201.8	a
nNOS/NOS Type I	a
p150Glued	a
p190-B	a
p47A-high	2.99
p68	a
Phosphotyrosine-PY20	a
pICln	4.07
PKA RI	a
PKA RII alpha	24.37
Psme3	30.62
Rabaptin-5	a
RACK1	10.82
Sam68	a
SHPS-1	a
Smad4/DPC4	a
SNX2	a
SRPK2	a
Stat3	28.24
Stat5	a
Stat5A	a
Striatin-high	a
TAF-172	a
TIAR	5.99
Tomosyn	a
Vti1a	a
Confidence level 4	
Cyclin A	3.60
DBP2	2.27
ENC-1	2.10
Endothelin 1 Receptor	3.37
LR11/SorLA/gp250	a
LXR	2.82
PKC iota	2.42
Skb1Hs	7.64

fold upregulation:
< 2
2-4
4-6
6-8
> 8
present

fold downregulation:
< 4
4-6
6-8
> 8
absent

Fig. 3 – Summary of protein changes after 15 h incubation with PSI. Protein changes are listed in the order of confidence. Changes greater than twofold in triplicate from good quality signals are of highest confidence (level 5), followed by changes 1.5–1.9-fold in triplicate from good quality signals (level 4). Protein changes obtained from weak signals although present in

Table 1 – List of proteins validated by conventional Western blotting

Protein ID	Changes		
	HL60	HL60/VCR	HL60/ADR
14-3-3	–	–	–
Bad	N/V	+	+
Bax	–	–	N/E
Bcl-2	0	0	0
Bid	–	–	–
Procaspase-3/CPP32	–	–	–
Procaspase-8	–	–	–
Jun	+	0	0
Phospho-JNK	+	0	0

(+), increase; (–), decrease, N/E, not expressed; 0, not changed; N/V, not validated.

mib, MG-132 lactacystin) were investigated. In addition, the levels of various proteins were modulated that are involved in cytoskeletal organization, potentially contributing to the morphological changes that are associated with apoptotic cell death (Annexin I, ABP280, AKAP149, CRP1, cdc42, DMPK, dystrobrevin, FLAP, MEK5a, PRK2/PAK2, Rac1, Rho, VASP). Also, the levels of several transcription factors including c-Jun, JAB1 (Jun activation domain-binding protein-1) were changed in PSI-treated cell lysates.

The fraction of proteins with altered expression levels, which are implicated in affecting apoptotic cell death are listed in supplementary Table S3. These proteins are involved in cell signaling, cell growth, cell adhesion, gene transcription, DNA repair, reactive oxygen generation, protein cleavage and other cellular processes. The levels of some of these proteins were modulated already 6 h following apoptosis induction by PSI and include proteins such as Bad, Cytochrome c, Hsp40, Jun and UbcH6, which were accumulated upon proteasome inhibition. In contrast, the level of other proteins such as ALDH, Bax, DFF45, DSIF, Eg5, FAK, FBP, XIAP, Integrin 5α, PTEN were significantly decreased under the same conditions (supplementary Table S3).

3.3. *Validation of PSI-induced modulation of protein levels using conventional immunoblotting analysis*

Conventional immunoblotting to reduce the probability of false positives was performed using antibodies obtained from alternative sources. Nine proteins critically involved in apoptosis regulation (Table 1) were selected to confirm their differential expression, results of which are presented in Fig. 5.

The activation of caspase cascade is a typical feature of apoptosis and the PowerBlot analysis accordingly had indicated a decrease of the proforms of several caspases, including caspases-2, -7, and -8, suggesting that these caspases became processed and activated. The presence of activated forms of caspases-3 and -8 were confirmed by conventional immunoblotting. Consistent with caspase-8 activation the amount of full-length caspase-8 substrate protein Bid was downregulated, suggesting that its proapoptotic truncated form tBid may contribute to the activation of the intrinsic (mitochondrial) apoptosis pathway. Bax levels appeared to be increased in contrast, although PowerBlot analysis had indicated a decrease in Bax protein levels. Strikingly, levels of Bad protein, a BH-3 only proapoptotic member of the Bcl-2 family proteins, were upregulated 18-fold and this accumulation of Bad was also apparent by conventional Western blotting. In contrast, 14-3-3 protein, an endogenous inhibitor of Bad function was reduced 4.7-fold as assessed by the PowerBlot analysis and also by subsequent conventional Western blotting. Our Western blotting analysis confirmed in addition upregulation of the phosphorylated form of JNK after incubation in HL-60 cells, arguing for activation of this pathway. Moreover, a 17-fold increased expression of the JNK substrate, c-Jun, was detected by the PowerBlot analysis and was also confirmed by conventional Western blotting. These results are in line with other observations suggesting that proteasome inhibitor mediated cell death is strongly dependent on activation of the JNK stress-signaling pathway [22,28].

3.4. *Analysis of selected proteins in multidrug-resistant HL-60 cell lines*

The consequences of PSI-administration were also examined in two drug-resistant HL-60 cell lines: HL-60/ADR cells are doxorubicin-resistant and overexpress the multidrug resistance-related protein (MRP) [45]. HL-60/VCR cells in contrast were established as vincristine-resistant cells and overexpress P-glycoprotein. Both multidrug-resistant cell lines show enhanced efflux rates of various agents and hence display resistance to multiple anticancer drugs [46]. Compared to their parental HL-60 cells, the MRP-expressing HL-60/ADR cells are about 122.5-, 14- and 8.5-fold more resistant to DOX, VCR and VBL, respectively. Moreover, HL-60/VCR cells showed 3300-, 1400- and 262-fold enhanced resistance to VCR, VBL and DOX, respectively (Wu et al., 2001 Oncogene 20:7006-7010, 2001). Treatment of HL-60/ADR and HL-60/VCR cells with 50 μM PSI for 15 h indicated that both cell lines were considerably more resistant to PSI-mediated apoptosis induction than the parental HL-60 cells. Both multidrug-resistant cell lines showed 35% apoptosis after 15 h in the presence of 50 μM PSI whereas HL-60 cells revealed an increase to 83% (Fig. 6A). To determine whether the relative levels of critical apoptosis regulators such as Bax, Bad, Bid, or Bcl-2 would change in the less sensitive HL-60/ADR and HL-60/VCR cells an analogous fashion compared to the parental HL-60 cells, lysates from PSI-treated HL-60/ADR and HL-60/VCR cells were analyzed by Western blotting as described for the parental HL-60 cells. As demonstrated in Fig. 6B, processing of caspases-3 and -8 activation as well as the processing of Bid occurred in multidrug-resistant HL-60 cells in a

all three runs, as well as changes >2-fold that were obtained in duplicate only are not listed (confidence levels 3–1). p, presence of a protein; quantification was impossible due to low signal in control sample; a, absence of a protein; quantification was impossible due to low signal in PSI-treated sample.

Protein	mean
Confidence level 5	
Annexin I	2.85
beta-Catenin	p
Cyclin D2	p
DMPK	p
DNA Topo I	6.82
eIF-6(31)	p
FKBP12	p
GRB2	5.01
Hsp40	20.63
JAK1-high	p
PKC alpha	2.59
PTP1C/SHP1(61)	4.34
Rin1-low	p
SCP3	p
Ubc9	p
VASP(47)	18.07
Confidence level 4	
CDC42	p
CUL-3	p
Cytochrome c	p
MnSOD	p
NHE-1	p
pan ERK-mid	p
Confidence level 3	
ABP-280	4.33
AF6	5.85
Annexin VI	6.35
BAF60a	3.60
BiP/GRP78	2.42
Flotillin-2/ESA	2.59
Fnk	4.34
GOK/Stim1	p
Jun	3.88
Ndr	2.36
p47A-low	1.82
PP1	1.92
PTP1C/SHP1(66)	3.09
Rab27	3.07
TRAX	2.03
Yes	2.87
Confidence level 2	
APM(46)	1.57
BPntase	p
Cyclin B	1.74
hcKrox	1.63
HEC	2.58
Integrin alpha 2/VLA-2	2.33
JAB1	1.77
LAP2-low	2.24
Lyn	p
p38 MAPK	2.30
PCMT-II	2.21
Phospholipase C delta 1	p
RAFT1/FRAP	1.81
Rho	p

Protein	mean
Confidence level 5	
Adaptin delta	3.77
AKAP149	a
Endopeptidase 3.4.24.16	29.63
FAK	a
FLAP	6.08
LR11/SorLA/gp250	a
PARP	a
PTEN	5.34
Reps1	a
Topo II alpha	a
Transportin	2.59
Confidence level 5	
Acetylcholinesterase	2.40
ALDH	a
Annexin IV	a
Caspase-3/CPP32	a
CDC42GAP	a
CUL-3	a
G protein beta	a
PRK2	a
SHPS-1	11.50
Confidence level 3	
Adaptin alpha	2.02
DAP3	2.57
DFF45	2.15
ECA39	2.79
hRAD9	2.52
La Protein	2.46
MCM6	4.74
Psme3	2.08
RanBP1	3.87
SRPK1	1.66
STI1	2.22
UBE3A	5.63
Confidence level 2	
Acetylcholine Receptor alpha	1.92
APM	1.94
c-Cbl	1.59
Eg5	2.19
ENC-1	1.70
FEN-1	2.16
GDNFR-alpha	2.47
HAX-1	2.06
HpRp16	a
Inhibitor 2	2.38
Integrin alpha v	6.86
MEK1	9.42
NAT1	a
PYK2/CAK beta	1.86
Rabaptin-5	30.30
RBBP	1.85
Spi	3.99
Stat3	a
Symplekin	a

fold upregulation:

< 2
2-4
4-6
6-8
> 8
present

fold downregulation:

< 4
4-6
6-8
> 8
absent

Fig. 4 – Summary of protein changes after 6 h incubation with PSI. See legend to Fig. 3.

comparable fashion, indicating that the apoptosis machinery still can be engaged in the drug resistant cells, albeit significantly higher concentrations of PSI were required to achieve this effect. Likewise, upregulation of Bad in the presence of reduced levels of 14-3-3 protein was also observed in the drug resistant cell lines.

The most striking differences between the HL-60 cells and their drug-resistant variants, however, pertained to the levels of Bax and to the differential activation of the JNK signaling pathway as determined by the extent of JNK phosphorylation, the total amount of JNK and the levels of c-Jun: in contrast to the drug sensitive parental HL-60 cells, which showed enhanced levels of total Bax protein, Bax appeared to be completely absent from HL-60/ADR and display a marked reduction in HL-60/VCR cells. In addition, there was no increase in JNK phosphorylation in both the HL-60/ADR and HL-60/VCR cells and c-Jun levels remained unaltered in contrast to the parental cells (compare with Fig. 5). These results suggested that lower levels of the proapoptotic Bax protein as well as the failure to activate JNK stress signaling might have contributed to the enhanced resistance to PSI-induced apoptosis.

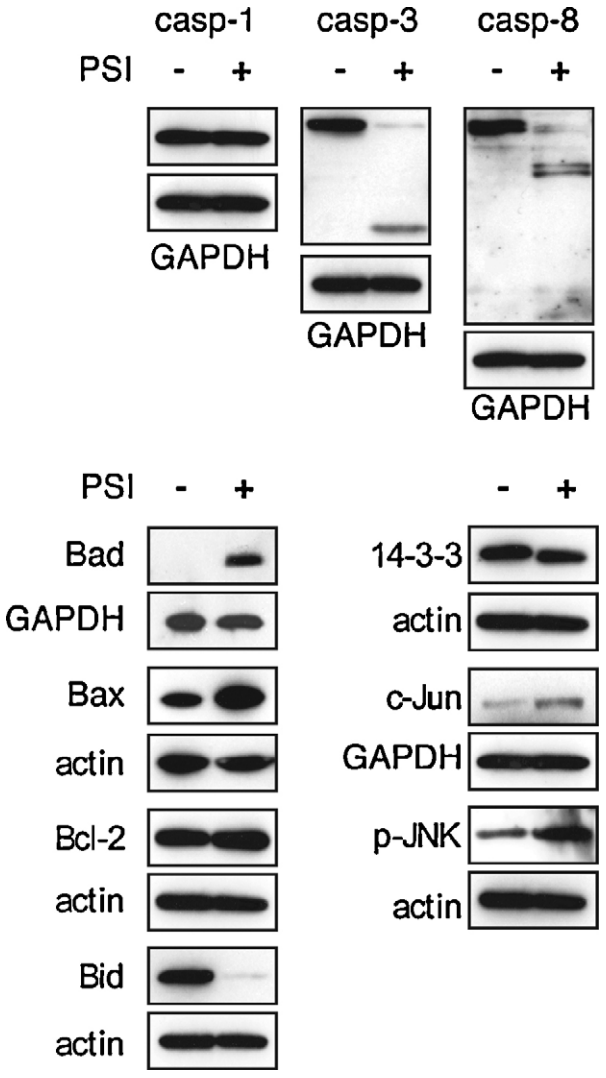

Fig. 5 – Conventional Western blotting to validate PowerBlot results. HL-60 cells were treated with 50 μM PSI for 15 h, lysed and subjected to analysis (40 μg protein/lane). Control cells received DMSO only and were processed under identical conditions. Anti-actin antibodies or anti-GAPDH antibodies were used to ensure equal loading. The membranes were developed with the chemiluminesence reagent SuperSignal West Pico (Pierce).

3.5. *P-glycoprotein and MRP-1-mediated efflux is not rate-limiting for PSI-mediated apoptosis in drug-resistant HL-60 cell lines*

The major mechanism of multidrug resistance in cancer cells is known to be increased efflux of drugs due to enhanced expression of ABC transporters, such as P-glycoprotein (P-gp) or the multidrug resistance associated protein 1 MRP-1, which act as drug efflux pumps. We therefore examined whether P-gp or MRP-1 would affect apoptosis induced by PSI in drug-resistant HL-60 cell lines by effectively lowering the intracellular concentrations of the proteasome inhibitor. To assess the relative contribution of both pumps, specific inhibitors of P-gp (PSC833) and of MRP-1 (MK571) were applied in combination with proteasome inhibitors. Application of PSC833 had no effect at all on HL-60/ADR cells and led only to a marginal increase of PSI-mediated apoptosis (+7.6%) in HL-60/VCR cells (Fig. 7). Similarly, MK571 only weakly increased PSI-mediated apoptosis in HL-60/ADR (+8.3%) and in HL-60/VCR cells (+7.4%) (Fig. 7). Both inhibitors did not show any effect on the drug-sensitive parental HL-60 cells when challenged with PSI (Fig. 7). These results demonstrated that pharmacological inhibition of the drug transporters only partially affected PSI-mediated apoptosis induction and that most likely only a minor part of the resistance to PSI stemmed from its lower accumulation within these cells.

4. Discussion

Microarray experiments have demonstrated that the transcriptional profile of a potentially large number of genes is changed in response to proteasome inhibition [6,47–49], however, only in a few instances transcriptional profiling was complemented with the analysis of changes instigated within the proteome of the treated cells [6,50]. In the present study we therefore compared the subproteome of cells induced to undergo apoptosis by treatment with the proteasome inhibitor PSI with the subproteome of control cells using a high throughput immunoblot screening procedure and attempted to define changes relevant for the regulation of apoptosis induction.

Consistent with the fact that PSI administration resulted in extensive apoptosis and caspase activation within a 24 h period, the proform of several caspases (caspases-3, -2, -7, -8) was downregulated after the administration of PSI, reflecting their processing and activation. While a significant contribution of the intrinsic apoptosis pathway to proteasome inhibitor mediated cell death is undisputed, the impact of the extrinsic apoptosis pathway involving death receptor activation by their corresponding ligands and caspase-8 activation is currently less clear. However, increased levels of TRADD, FADD, Fas and FasL in PSI-treated HL60 cells supported a role of the extrinsic pathway of apoptosis, and sensitization of various tumor cell lines to TRAIL-induced apoptosis by the proteasome inhibitor bortezomib has been reported, which is due to upregulation of TRAIL itself as well as of its receptor Decoy receptor 5 (DR5) [51,52]. Thus, administration of proteasome inhibitors results in the stimulation of a pro-apoptotic autocrine loop by signaling via death receptor family members. However, as Milner et al. had shown previously [53], genotoxic stress induced by chemotherapeutic drugs can differentially upregulate TRAIL, TNF and CD95L and activate caspase-8 in a FADD-independent manner without engagement of their receptor partners.

In parallel to the caspase activation, relative levels of various proteins known to be processed by activated executioner caspases decreased, e.g. DNA fragmentation factor (DFF-45) and PARP, which become processed by caspase-3. Similarly, STAT3 and STAT5 levels were diminished in lysates from PSI-treated cells, which also could be due to caspase mediated cleavage [54], whereas STAT1, which has been described as a caspase substrate by King et al. in contrast showed increased levels in our hands [55]. Additional studies

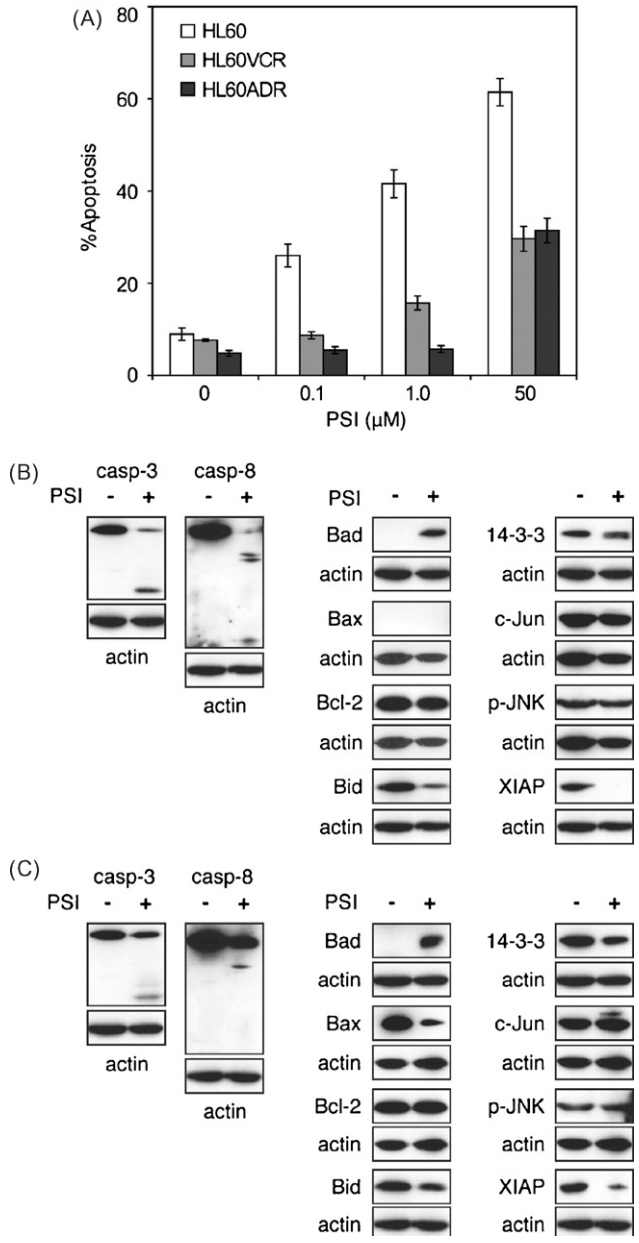

Fig. 6 – Proteasome inhibitor-mediated apoptosis induction in drug-resistant HL-60 cells. (A) Vincristine-resistant HL-60 cells as well as doxorubicin-resistant HL-60 cells were treated with PSI for 15 h with 50 μM PSI. The extent of apoptosis induction was analyzed by flow cytometry after staining the cells with Annexin-V-FITC and PI. The sum of percentages of early (Annexin-V-FITC$^+$ and PI$^-$) and late (Annexin-V-FITC$^+$ and PI$^+$) apoptotic cells are presented as %apoptosis. Shown are the mean values of six independent experiments. Expression levels of selected proteins modulated in HL-60 cells during PSI-mediated apoptosis were analyzed in doxorubicin resistant HL-60/ADR cells (B) and vincristine-resistant HL-60/VCR cells (C). The cells were treated with 50 μM PSI for 15 h (+) and 40 μg of total protein were subjected to Western blotting analysis. Control cells received DMSO only (−). To check for equal loading each blot was reprobed with anti-actin antibodies. The membranes were developed with the chemiluminesence reagent SuperSignal West Pico (Pierce). Representative blots from three experiments are shown.

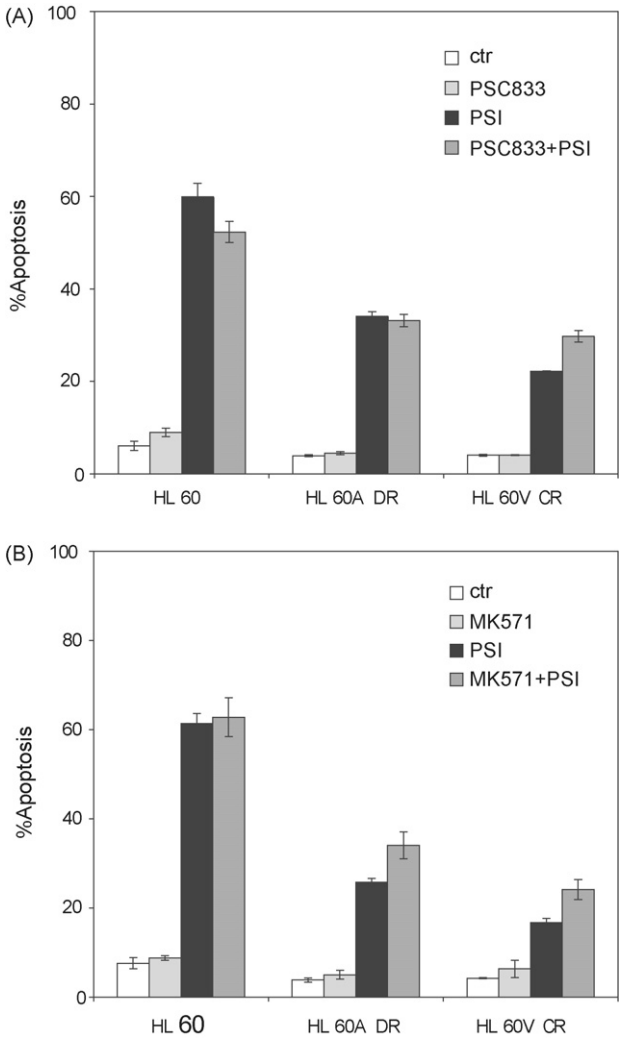

Fig. 7 – P-glycoprotein and multidrug resistance associated proteins barely limit PSI-mediated apoptosis in drug-resistant HL-60 cell lines. HL-60/ADR cells and HL-60/VCR cells were preincubated with either 3 μM of P-gp inhibitor PSC833 (A) or 30 μM of MRP-1 inhibitor MK571 (B). Cells were treated for 15 h with MDR inhibitors only (light gray bar), with 50 μM PSI only (black bar) or with both MDR inhibitors and PSI together (dark gray bar). Apoptosis induction was analyzed by flow cytometry after staining the cells with Annexin-V-FITC and PI. Total amount of apototic cells are presented as sum of percentages of early (Annexin-V-FITC$^+$ and PI$^-$) and late (Annexin-V-FITC$^+$ and PI$^+$) apoptosis. Shown are the mean values of six independent experiments.

are required to determine whether STAT1 turnover is subject to rapid proteasomal degradation and/or is rendered inaccessible for active caspases in the presence of PSI. The PowerBlot analysis demonstrated in addition a fourfold decrease of the inhibitor of apoptosis hILP/XIAP protein during PSI-mediated

apoptosis. XIAP is prone to caspase-mediated cleavage, which yields an N-terminal fragment that blocks caspases-3 and -7 activity and a C-terminal fragment, which inhibits caspase-9 [56], suggesting that XIAP levels become reduced because of caspase-mediated cleavage. However, expression of XIAP is regulated in addition by transactivation of NFκB, whose activation is controlled by proteasome function [57]. In summary, these results demonstrated that signature events of apoptosis induction were present in PSI-treated HL-60 cells.

When comparing alterations of selected apoptosis regulators, which showed significant changes in HL60 cells with the corresponding changes in two multidrug-resistant HL-60 variant cell lines, it became apparent that activation of caspases-3 and -8, although possible, did not occur to the same extent as in PSI-sensitive HL60 cells (compare Figs. 5 and 6). Caspase-3 activation was reduced in both multidrug-resistant cell lines and caspase-8 activation was particularly lower in HL-60/VCR cells, which correlated well with the reduced extent of apoptosis induction in both resistant cell lines (Fig. 6A) and the processing of Bid.

Prominent accumulation of Bad, which is a pro-apoptotic BH3-only member of the Bcl-2 family proteins, was observed in all three cell lines. Two PEST sequences predicted by the "PEST find" algorithm to be present in the amino acid sequence of Bad (amino acids 1–20 and 73–94 in human Bad and amino acids 37–62 and 110–131 in mouse Bad) supported the notion that Bad could be a potential substrate of the ubiquitin–proteasome pathway and that its accumulation is a consequence of proteasome inhibition. Accumulation of Bad in three different cell lines upon administration of proteasome inhibitor is a novel finding and has not been reported so far. These changes, which would argue for an increased sensitization of the cells to proteasome inhibitor-mediated apoptosis did, however, not match the measured extent of apoptosis induction in the three cell lines. We therefore concluded, that a shift in the balance between Bad and 14-3-3 protein levels towards increased amounts of Bad was not a crucial parameter in determining the sensitivity for apoptosis induction by PSI and that other factors contribute to this process. The levels of the apoptosis initiator Bax, e.g. correlated inversely with the inclination of the cells to initiate apoptosis, Bax was readily detected in the parental HL-60 cells, however, Bax levels were low or even absent in the drug-resistant cell lines, suggesting the levels of this protein could be an important parameter determining the differential sensitivity towards PSI-induced apoptosis. Further experiments involving, e.g. siRNA-mediated knockdown of Bax in the parental cells could address this hypothesis in more detail.

An equally obvious correlation between alterations in protein levels and the extent of apoptosis induction was noticed for the phosphorylated form of JNK: While the degree of JNK phosphorylation increased in the HL-60 parental cells, it remained unchanged in both drug resistant cell lines, suggesting that drug resistance in these cells could be based on the failure to activate the JNK stress signaling pathway.

These paradigms demonstrate that the proteome composition upon exposure to proteasome inhibitors is not only affected by changes on a transcriptional level as can be determined by microarray experiments, but is in the first line the result of post-translational events, such as inhibition of protein turnover and protein accumulation, modification by phosphorylation and ubiquitin conjugation as well as proteolytic processing by caspases [58,59]. To delineate critical events in cellular signaling that ultimately lead to the demise of leukemic cells by proteasome inhibitors, it is therefore essential to complement mRNA expression studies with a characterization of changes within the proteome.

Our results suggest that resistance to PSI was in part due to reduced intracellular amounts of the proteasome inhibitor due to increased drug efflux in the MDR-1 and MRP-1 expressing cells, which may have been the reason for the lack of JNK activation in both cell lines and the reduced sensitivity to undergo apoptosis. However, since blocking the function of P-gp or MRP-1 by pharmacological means did not seem to exhaustively resensitize the drug resistant HL-60 cell lines to PSI treatment (Fig. 7), these results suggest that the intracellular levels of the proteasome inhibitor PSI are not affected by P-gp or MRP-1-mediated drug efflux in HL-60 cells. Conflicting data have been reported regarding the significance of P-gp or MDR-1 expression on resistance to proteasome inhibitor treatment [60,61], and it will be important to determine whether these differences are due to distinct proteasome inhibitors investigated [60] or to cell type specific differences.

Proteasome function is essential for cellular survival and it is therefore conceivable that tumor cells may have adopted failsafe mechanisms to compensate for the inhibitor-induced loss of functional proteasome particles. Multiple myeloma cells have thus been reported to upregulate various proteasomal subunits in response to bortezomib treatment [59], which in conjunction with an altered subunit composition may result in increased overall catabolic activity by the ubiquitin–proteasome pathway. Similar observations were also made in Burkitt lymphoma [62] and in vascular smooth muscle cells [63]. In addition upregulation of heat shock proteins is a characteristic feature of tumor cells that have acquired a drug resistant phenotype and Chuahan et al. indeed demonstrated that the blockage of Hsp27 is sufficient to resensitize bortezomib-resistant lymphoma cells to proteasome inhibitor-mediated cytotoxicity [64]. Tumor cells may also escalate protein removal via alternative routes such as lysosomal degradation or autophagy during conditions of proteasomal blockage to reduce the load of accumulating proteins [65]. Drug resistance has become an important issue since, e.g. only a fraction of the multiple myeloma patients that receives treatment with the proteasome inhibitor bortezomib is responding to drug treatment and tumor cells resistant to bortezomib may be also cross-resistant to other cytotoxic compounds [61]. Here we have shown that expression of multidrug proteins and drug efflux pump activity is irrelevant for the resistance to the cytotoxic effect of PSI. Our observations will now allow the focused identification of alternative mechanisms responsible for the resistance to proteasome inhibitor-mediated apoptosis.

Acknowledgements

This work was supported by National Cancer Institute Grants CA 90878, CA 080734, and CA 101743 (to A.R.S.) and by the Max Planck Society (H.C.A.D.).

Appendix A. Supplementary data

Supplementary data associated with this article can be found, in the online version, at doi:10.1016/j.bcp.2008.03.017.

REFERENCES

[1] Drexler HC. Activation of the cell death program by inhibition of proteasome function. Proc Natl Acad Sci USA 1997;94(3):855–60.
[2] An B, Goldfarb RH, Siman R, Dou QP. Novel dipeptidyl proteasome inhibitors overcome Bcl-2 protective function and selectively accumulate the cyclin-dependent kinase inhibitor p27 and induce apoptosis in transformed, but not normal, human fibroblasts. Cell Death Differ 1998;5(12):1062–75.
[3] Drexler HC, Pebler S. Inducible p27(Kip1) expression inhibits proliferation of K562 cells and protects against apoptosis induction by proteasome inhibitors. Cell Death Differ 2003;10(3):290–301.
[4] Delic J, Masdehors P, Omura S, Cosset JM, Dumont J, Binet JL, et al. The proteasome inhibitor lactacystin induces apoptosis and sensitizes chemo- and radioresistant human chronic lymphocytic leukaemia lymphocytes to TNF-alpha-initiated apoptosis. Br J Cancer 1998;77(7):1103–7.
[5] Amiri KI, Horton LW, LaFleur BJ, Sosman JA, Richmond A. Augmenting chemosensitivity of malignant melanoma tumors via proteasome inhibition: implication for bortezomib (VELCADE, PS-341) as a therapeutic agent for malignant melanoma. Cancer Res 2004;64(14):4912–8.
[6] Mitsiades N, Mitsiades CS, Richardson PG, Poulaki V, Tai YT, Chauhan D, et al. The proteasome inhibitor PS-341 potentiates sensitivity of multiple myeloma cells to conventional chemotherapeutic agents: therapeutic applications. Blood 2003;101(6):2377–80.
[7] An WG, Hwang SG, Trepel JB, Blagosklonny MV. Protease inhibitor-induced apoptosis: accumulation of wt p53, p21WAF1/CIP1, and induction of apoptosis are independent markers of proteasome inhibition. Leukemia 2000;14(7):1276–83.
[8] Dai Y, Rahmani M, Pei XY, Dent P, Grant S. Bortezomib and flavopiridol interact synergistically to induce apoptosis in chronic myeloid leukemia cells resistant to imatinib mesylate through both Bcr/Abl-dependent and -independent mechanisms. Blood 2004;104(2):509–18.
[9] Oyaizu H, Adachi Y, Okumura T, Okigaki M, Oyaizu N, Taketani S, et al. Proteasome inhibitor 1 enhances paclitaxel-induced apoptosis in human lung adenocarcinoma cell line. Oncol Rep 2001;8(4):825–9.
[10] Yu C, Rahmani M, Conrad D, Subler M, Dent P, Grant S. The proteasome inhibitor bortezomib interacts synergistically with histone deacetylase inhibitors to induce apoptosis in Bcr/Abl+ cells sensitive and resistant to STI571. Blood 2003;102(10):3765–74.
[11] Drexler HC, Euler M. Synergistic apoptosis induction by proteasome and histone deacetylase inhibitors is dependent on protein synthesis. Apoptosis 2005;10(4):743–58.
[12] Orlowski RZ, Eswara JR, Lafond-Walker A, Grever MR, Orlowski M, Dang CV. Tumor growth inhibition induced in a murine model of human Burkitt's lymphoma by a proteasome inhibitor. Cancer Res 1998;58(19):4342–8.
[13] Teicher BA, Ara G, Herbst R, Palombella VJ, Adams J. The proteasome inhibitor PS-341 in cancer therapy. Clin Cancer Res 1999;5(9):2638–45.
[14] Adams J, Palombella VJ, Sausville EA, Johnson J, Destree A, Lazarus DD, et al. Proteasome inhibitors: a novel class of potent and effective antitumor agents. Cancer Res 1999;59(11):2615–22.
[15] Adams J. The proteasome: a suitable antineoplastic target. Nat Rev Cancer 2004;4(5):349–60.
[16] Richardson PG. A review of the proteasome inhibitor bortezomib in multiple myeloma. Expert Opin Pharmacother 2004;5(6):1321–31.
[17] Chauhan D, Catley L, Li G, Podar K, Hideshima T, Velankar M, et al. A novel orally active proteasome inhibitor induces apoptosis in multiple myeloma cells with mechanisms distinct from Bortezomib. Cancer Cell 2005;8(5):407–19.
[18] Chauhan D, Hideshima T, Anderson KC. A novel proteasome inhibitor NPI-0052 as an anticancer therapy. Br J Cancer 2006;95(8):961–5.
[19] Demo SD, Kirk CJ, Aujay MA, Buchholz TJ, Dajee M, Ho MN, et al. Antitumor activity of PR-171, a novel irreversible inhibitor of the proteasome. Cancer Res 2007;67(13):6383–91.
[20] Ling YH, Liebes L, Jiang JD, Holland JF, Elliott PJ, Adams J, et al. Mechanisms of proteasome inhibitor PS-341-induced G(2)-M-phase arrest and apoptosis in human non-small cell lung cancer cell lines. Clin Cancer Res 2003;9(3):1145–54.
[21] Pei XY, Dai Y, Grant S. The proteasome inhibitor bortezomib promotes mitochondrial injury and apoptosis induced by the small molecule Bcl-2 inhibitor HA14-1 in multiple myeloma cells. Leukemia 2003;17(10):2036–45.
[22] Hideshima T, Mitsiades C, Akiyama M, Hayashi T, Chauhan D, Richardson P, et al. Molecular mechanisms mediating antimyeloma activity of proteasome inhibitor PS-341. Blood 2003;101(4):1530–4.
[23] Yang Y, Ikezoe T, Saito T, Kobayashi M, Koeffler HP, Taguchi H. Proteasome inhibitor PS-341 induces growth arrest and apoptosis of non-small cell lung cancer cells via the JNK/c-Jun/AP-1 signaling. Cancer Sci 2004;95(2):176–80.
[24] Chauhan D, Li G, Podar K, Hideshima T, Mitsiades C, Schlossman R, et al. Targeting mitochondria to overcome conventional and bortezomib/proteasome inhibitor PS-341 resistance in multiple myeloma (MM) cells. Blood 2004;104(8):2458–66.
[25] Ishizawa J, Yoshida S, Oya M, Mizuno R, Shinojima T, Marumo K, et al. Inhibition of the ubiquitin–proteasome pathway activates stress kinases and induces apoptosis in renal cancer cells. Int J Oncol 2004;25(3):697–702.
[26] Dai Y, Rahmani M, Grant S. Proteasome inhibitors potentiate leukemic cell apoptosis induced by the cyclin-dependent kinase inhibitor flavopiridol through a SAPK/JNK- and NF-kappaB-dependent process. Oncogene 2003;22(46):7108–22.
[27] Orlowski RZ, Small GW, Shi YY. Evidence that inhibition of p44/42 mitogen-activated protein kinase signaling is a factor in proteasome inhibitor-mediated apoptosis. J Biol Chem 2002;277(31):27864–71.
[28] Yu C, Rahmani M, Dent P, Grant S. The hierarchical relationship between MAPK signaling and ROS generation in human leukemia cells undergoing apoptosis in response to the proteasome inhibitor Bortezomib. Exp Cell Res 2004;295(2):555–66.
[29] Wang CY, Mayo MW, Korneluk RG, Goeddel DV, Baldwin ASJ. NF-kappaB antiapoptosis: induction of TRAF1 and TRAF2 and c-IAP1 and c-IAP2 to suppress caspase-8 activation. Science 1998;281(5383):1680–3.
[30] Stehlik C, de Martin R, Kumabashiri I, Schmid JA, Binder BR, Lipp J. Nuclear factor (NF)-kappaB-regulated X-chromosome-linked iap gene expression protects endothelial cells from tumor necrosis factor alpha-induced apoptosis. J Exp Med 1998;188(1):211–6.

[31] Zong WX, Edelstein LC, Chen C, Bash J, Gelinas C. The prosurvival Bcl-2 homolog Bfl-1/A1 is a direct transcriptional target of NF-kappaB that blocks TNFalpha-induced apoptosis. Genes Dev 1999;13(4):382–7.
[32] Hu X, Yee E, Harlan JM, Wong F, Karsan A. Lipopolysaccharide induces the antiapoptotic molecules, A1 and A20, in microvascular endothelial cells. Blood 1998;92(8):2759–65.
[33] Bui NT, Livolsi A, Peyron JF, Prehn JH. Activation of nuclear factor kappaB and Bcl-x survival gene expression by nerve growth factor requires tyrosine phosphorylation of IkappaBalpha. J Cell Biol 2001;152(4):753–64.
[34] Chen Z, Hagler J, Palombella VJ, Melandri F, Scherer D, Ballard D, et al. Signal-induced site-specific phosphorylation targets I kappa B alpha to the ubiquitin–proteasome pathway. Genes Dev 1995;9(13):1586–97.
[35] Palombella VJ, Rando OJ, Goldberg AL, Maniatis T. The ubiquitin–proteasome pathway is required for processing the NF-kappa B1 precursor protein and the activation of NF-kappa B. Cell 1994;78(5):773–85.
[36] Courtois G, Gilmore TD. Mutations in the NF-kappaB signaling pathway: implications for human disease. Oncogene 2006;25(51):6831–43.
[37] Annunziata CM, Davis RE, Demchenko Y, Bellamy W, Gabrea A, Zhan F, et al. Frequent engagement of the classical and alternative NF-kappaB pathways by diverse genetic abnormalities in multiple myeloma. Cancer Cell 2007;12(2):115–30.
[38] Keats JJ, Fonseca R, Chesi M, Schop R, Baker A, Chng WJ, et al. Promiscuous mutations activate the noncanonical NF-kappaB pathway in multiple myeloma. Cancer Cell 2007;12(2):131–44.
[39] Xu H, Ju D, Jarois T, Xie Y. Diminished feedback regulation of proteasome expression and resistance to proteasome inhibitors in breast cancer cells. Breast Cancer Res Treat 2007.
[40] Davis NB, Taber DA, Ansari RH, Ryan CW, George C, Vokes EE, et al. Phase II trial of PS-341 in patients with renal cell cancer: a University of Chicago phase II consortium study. J Clin Oncol 2004;22(1):115–9.
[41] Wolter KG, Verhaegen M, Fernandez Y, Nikolovska-Coleska Z, Riblett M, de la Vega CM, et al. Therapeutic window for melanoma treatment provided by selective effects of the proteasome on Bcl-2 proteins. Cell Death Differ 2007;14(9):1605–16.
[42] Cheriyath V, Jacobs BS, Hussein MA. Proteasome inhibitors in the clinical setting: benefits and strategies to overcome multiple myeloma resistance to proteasome inhibitors. Drugs R D 2007;8(1):1–12.
[43] McGrath T, Latoud C, Arnold ST, Safa AR, Felsted RL, Center MS. Mechanisms of multidrug resistance in HL60 cells. Analysis of resistance associated membrane proteins and levels of mdr gene expression. Biochem Pharmacol 1989;38(20):3611–9.
[44] Ogretmen B, Safa AR. Identification and characterization of the MDR1 promoter-enhancing factor 1 (MEF1) in the multidrug resistant HL60/VCR human acute myeloid leukemia cell line. Biochemistry 2000;39(1):194–204.
[45] Ross DD, Doyle LA, Yang W, Tong Y, Cornblatt B. Susceptibility of idarubicin, daunorubicin, and their C-13 alcohol metabolites to transport-mediated multidrug resistance. Biochem Pharmacol 1995;50(10):1673–83.
[46] Wu CH, Rastegar M, Gordon J, Safa AR. Beta(2)-microglobulin induces apoptosis in HL-60 human leukemia cell line and its multidrug resistant variants overexpressing MRP1 but lacking Bax or overexpressing P-glycoprotein. Oncogene 2001;20(48):7006–20.
[47] Carreras I, Garrett-Young R, Ullman MD, Eisenhauer PB, Fine RE, Wells JM, et al. Upregulation of clusterin/apolipoprotein J in lactacystin-treated SH-SY5Y cells. J Neurosci Res 2005;79(4):495–502.
[48] Landowski TH, Megli CJ, Nullmeyer KD, Lynch RM, Dorr RT. Mitochondrial-mediated disregulation of Ca^{2+} is a critical determinant of Velcade (PS-341/bortezomib) cytotoxicity in myeloma cell lines. Cancer Res 2005;65(9):3828–36.
[49] Yew EH, Cheung NS, Choy MS, Qi RZ, Lee AY, Peng ZF, et al. Proteasome inhibition by lactacystin in primary neuronal cells induces both potentially neuroprotective and pro-apoptotic transcriptional responses: a microarray analysis. J Neurochem 2005;94(4):943–56.
[50] Jin BF, He K, Wang HX, Wang J, Zhou T, Lan Y, et al. Proteomic analysis of ubiquitin–proteasome effects: insight into the function of eukaryotic initiation factor 5A. Oncogene 2003;22(31):4819–30.
[51] He Q, Huang Y, Sheikh MS. Proteasome inhibitor MG132 upregulates death receptor 5 and cooperates with Apo2L/TRAIL to induce apoptosis in Bax-proficient and -deficient cells. Oncogene 2004;23(14):2554–8.
[52] Johnson TR, Stone K, Nikrad M, Yeh T, Zong WX, Thompson CB, et al. The proteasome inhibitor PS-341 overcomes TRAIL resistance in Bax and caspase 9-negative or Bcl-xL overexpressing cells. Oncogene 2003;22(32):4953–63.
[53] Milner AE, Palmer DH, Hodgkin EA, Eliopoulos AG, Knox PG, Poole CJ, et al. Induction of apoptosis by chemotherapeutic drugs: the role of FADD in activation of caspase-8 and synergy with death receptor ligands in ovarian carcinoma cells. Cell Death Differ 2002;9(3):287–300.
[54] Darnowski JW, Goulette FA, Guan YJ, Chatterjee D, Yang ZF, Cousens LP, et al. Stat3 cleavage by caspases: impact on full-length Stat3 expression, fragment formation, and transcriptional activity. J Biol Chem 2006;281(26):17707–1.
[55] King P, Goodbourn S. STAT1 is inactivated by a caspase. J Biol Chem 1998;273(15):8699–704.
[56] Deveraux QL, Leo E, Stennicke HR, Welsh K, Salvesen GS, Reed JC. Cleavage of human inhibitor of apoptosis protein XIAP results in fragments with distinct specificities for caspases. EMBO J 1999;18(19):5242–51.
[57] Piva R, Gianferretti P, Ciucci A, Taulli R, Belardo G, Santoro MG. 15-Deoxy-delta 12, 14-prostaglandin J2 induces apoptosis in human malignant B cells: an effect associated with inhibition of NF-kappa B activity and down-regulation of antiapoptotic proteins. Blood 2005;105(4):1750–8.
[58] Voortman J, Resende TP, Abou El Hassan MA, Giaccone G, Kruyt FA. TRAIL therapy in non-small cell lung cancer cells: sensitization to death receptor-mediated apoptosis by proteasome inhibitor bortezomib. Mol Cancer Ther 2007;6(7):2103–12.
[59] Mitsiades N, Mitsiades CS, Poulaki V, Chauhan D, Fanourakis G, Gu X, et al. Molecular sequelae of proteasome inhibition in human multiple myeloma cells. Proc Natl Acad Sci USA 2002;99(22):14374–9.
[60] Minderman H, Zhou Y, O'Loughlin KL, Baer MR. Bortezomib activity and in vitro interactions with anthracyclines and cytarabine in acute myeloid leukemia cells are independent of multidrug resistance mechanisms and p53 status. Cancer Chemother Pharmacol 2007;60(2):245–55.
[61] Nakamura T, Tanaka K, Matsunobu T, Okada T, Nakatani F, Sakimura R, et al. The mechanism of cross-resistance to proteasome inhibitor bortezomib and overcoming resistance in Ewing's family tumor cells. Int J Oncol 2007;31(4):803–11.
[62] Fuchs D, Berges C, Opelz G, Daniel V, Naujokat C. Increased expression and altered subunit composition of proteasomes induced by continuous proteasome inhibition establish apoptosis resistance and hyperproliferation of Burkitt lymphoma cells. J Cell Biochem 2007.
[63] Meiners S, Heyken D, Weller A, Ludwig A, Stangl K, Kloetzel PM, et al. Inhibition of proteasome activity induces

concerted expression of proteasome genes and de novo formation of Mammalian proteasomes. J Biol Chem 2003;278(24):21517–25.
[64] Chauhan D, Li G, Shringarpure R, Podar K, Ohtake Y, Hideshima T, et al. Blockade of Hsp27 overcomes Bortezomib/proteasome inhibitor PS-341 resistance in lymphoma cells. Cancer Res 2003;63(19):6174–7.
[65] Ding WX, Ni HM, Gao W, Yoshimori T, Stolz DB, Ron D, et al. Linking of autophagy to ubiquitin–proteasome system is important for the regulation of endoplasmic reticulum stress and cell viability. Am J Pathol 2007;171(2):513–24.